Osteochondral Defect Repair Using Bilayered Implants Of Additively Manufactured Biodegradable Porous Zinc And Chondroitin Sulfate.

Holger Jahr (1), Fan Yang (2), Yageng Li (3), Lei Wang (3), Haodong Che (3), Xin Zhang (2), Luning Wang (3), Dong Jiang, Hongjie Huang and Jianquan Wang (2)

(1) University Hospital RWTH Aachen and Institute of Structural Mechanics and Lightweight Design, RWTH Aachen University, 52062, Aachen, Germany; (2) *Department of Sports Medicine, Peking University Third Hospital, Institute of Sports Medicine of Peking University, Beijing Key Laboratory of Sports Injuries, Engineering Research Center of Sports Trauma Treatment Technology and Devices, Ministry of Education, Beijing, China* (3) *Beijing Advanced Innovation Center for Materials Genome Engineering, State Key Laboratory for Advanced Metals and Materials, School of Materials Science and Engineering, University of Science and Technology Beijing, Beijing, China.*

Introduction: Regeneration of osteochondral tissue requires the re-establishment of a gradient owing to the unique characteristics and healing potential of the chondral and osseous phases. Due to its limited self-healing capacity, for hyaline cartilage timely mechanical support during the regeneration period is crucial to achieving an efficient repair.
Methods: We created a biodegradable bilayered scaffold, comprising a chondroitin sulfate (CS) hydrogel to regenerate cartilaginous tissue and an additively manufactured (AM) porous pure zinc (Zn) scaffold to support subchondral bone repair.
Results: Our photocured CS hydrogel possesses a compressive strength of 82 kPa. The AM porous Zn scaffold exhibits a yield strength of 11 MPa and a stiffness of 0.8 GPa, respectively, which are values similar to those reported for cancellous bone. We demonstrate a favorable cytocompatibility and a facilitation of chondrogenic and osteogenic differentiation of bone marrow stem cells in vitro. In a porcine model, our scaffold supports simultaneous bone- and cartilage-like tissue regeneration, resulting in (i) a smoother cartilage surface, (ii) improved hyaline-like cartilage tissue formation, and (iii) a superior integration into the adjacent host tissue.
Discussion: Our ex vivo data on cytocompatibility and mechanical properties justified a subsequent in vivo trial in a relevant large animal model.
Significance/Clinical Relevance: Our results strongly suggest that this bilayered scaffold holds significant potential for clinical application in osteochondral regeneration.

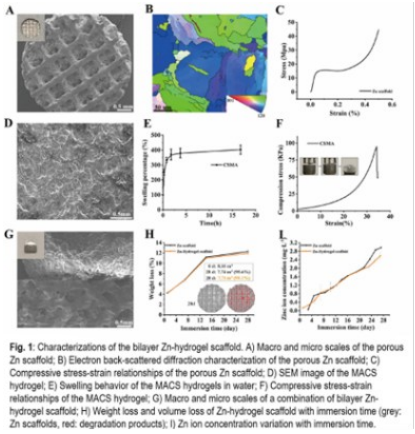

Fig. 1: Characterizations of the bilayer Zn-hydrogel scaffold. A) Macro and micro scales of the porous Zn scaffold; B) Electron back-scattered diffraction characterization of the porous Zn scaffold; C) Compressive stress-strain relationships of the porous Zn scaffold; D) SEM image of the MACS hydrogel; E) Swelling behavior of the MACS hydrogels in water; F) Compressive stress-strain relationships of the MACS hydrogel; G) Macro and micro scales of a combination of bilayer Zn-hydrogel scaffold; H) Weight loss and volume loss of Zn-hydrogel scaffold with immersion time (grey: Zn scaffolds, red: degradation products); I) Zn ion concentration variation with immersion time.

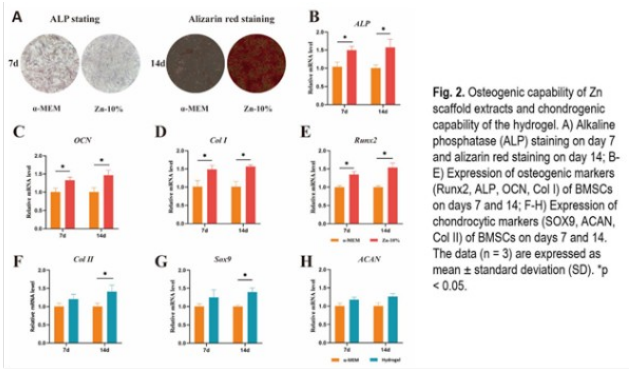

Fig. 2. Osteogenic capability of Zn scaffold extracts and chondrogenic capability of the hydrogel. A) Alkaline phosphatase (ALP) staining on day 7 and alizarin red staining on day 14; B-E) Expression of osteogenic markers (Runx2, ALP, OCN, Col I) of BMSCs on days 7 and 14; F-H) Expression of chondrocytic markers (SOX9, ACAN, Col II) of BMSCs on days 7 and 14. The data (n = 3) are expressed as mean ± standard deviation (SD). *p < 0.05.

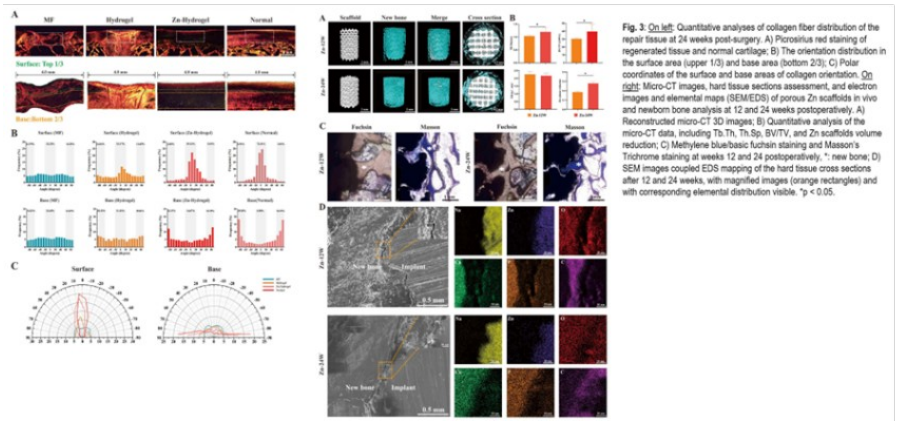

Fig. 3: On left: Quantitative analyses of collagen fiber distribution of the repair tissue at 24 weeks post-surgery. A) Picrosirius red staining of regenerated tissue and normal cartilage; B) The orientation distribution in the surface area (upper 1/3) and base area (bottom 2/3); C) Polar coordinates of the surface and base areas of collagen orientation. On right: Micro-CT images, hard tissue sections assessment, and electron images and elemental maps (SEM/EDS) of porous Zn scaffolds in vivo and newborn bone analysis at 12 and 24 weeks postoperatively. A) Reconstructed micro-CT 3D images; B) Quantitative analysis of the micro-CT data, including Tb.Th, Th.Sp, BV/TV, and Zn scaffolds volume reduction; C) Methylene blue/basic fuchsin staining and Masson's Trichrome staining at weeks 12 and 24 postoperatively, *: new bone; D) SEM images coupled EDS mapping of the hard tissue cross sections after 12 and 24 weeks, with magnified images (orange rectangles) and with corresponding elemental distribution visible. *p < 0.05.